Available online at www.sciencedirect.com
ScienceDirect
Nuclear Physics B Proceedings Supplement 00 (2014) 1–6
Nuclear Physics B Proceedings Supplement

Effective Spectral Function for Quasielastic Scattering on Nuclei from Deuterium to Lead

A. Bodek[a], M. E. Christy[b], B. Coopersmith[a]

[a]*Department of Physics and Astronomy, University of Rochester, Rochester, NY. 14627, USA*
[b]*Department of Physics, Hampton University, Hampton, Virginia, 23668 USA*
Presented by A. Bodek at the 37th International Conference on High Energy Physics (ICHEP 2014, 2-9 Jul 2014. Valencia, Spain, [C14-07-02])

arXiv:1409.8545v1 [nucl-th] 30 Sep 2014

Abstract

Spectral functions do not fully describe quasielastic electron and neutrino scattering from nuclei because they only model the initial state. Final state interactions distort the shape of the differential cross section at the peak and increase the cross section at the tails of the distribution. We show that the kinematic distributions predicted by the ψ' superscaling formalism can be well described with a modified *effective spectral function* (ESF). By construction, models using ESF in combination with the transverse enhancement contribution correctly predict electron QE scattering data. Our values for the binding energy parameter Δ are smaller than $\overline{\epsilon}$ extracted within the Fermi gas model from pre 1971 data by Moniz[8], probably because these early cross sections were not corrected for coulomb effects.

Keywords: Spectral Functions Quasielastic Electron Scattering Neutrino Scattering

1. Introduction

Neutrino oscillation experiments make use of neutrino Monte Carlo (MC) event generators to model the cross sections and kinematic distributions of the leptonic and hadronic final state of neutrino interactions on nuclear targets. Because of the conservation of the vector current (CVC), the same models should be able to reliably predict the quasielaststic electron scattering cross section on nuclear targets. Unfortunately, none of the models that are currently implemented in neutrino MC generators are able to do it. Here we summarize an approach which guarantees agreement with QE electron scattering data by construction. A more detailed description is given in reference [1]

The left panel of Fig. 1 is the general diagram for QE lepton (election, muon or neutrino) scattering from a nucleon which is bound in a nucleus of mass M_A. In this paper, we focus on charged current neutrino scattering. The scattering is from an off-shell bound neutron of momentum $\mathbf{P_i} = \mathbf{k}$. The on-shell recoil $[A-1]^*$ (spectator) nucleus has a momentum $\mathbf{P^*_{A-1}} = \mathbf{P_s} = -\mathbf{k}$. This process is referred to as the 1p1h process (one proton one hole). The * is used to indicate that the spectator nucleus is not in the ground state because it has one hole. The four-momentum transfer to the nuclear target is defined as $q = (\vec{q}, \nu)$. Here ν is the energy transfer, and $Q^2 = -q^2 = \nu^2 - \vec{q}^2$ is the square of the four-momentum transfer. For free nucleons the energy transfer ν is equal to $Q^2/2M_N$ where M_N is the mass of the nucleon. At a fixed value of Q^2, QE scattering on nucleons bound in a nucleus yields a distribution in ν which peaks at $\nu = Q^2/2M_N$. In this communication, the term "normalized quasielastic distribution" refers to the normalized differential cross section $\frac{1}{\sigma}\frac{d\sigma}{d\nu}(Q^2,\nu) = \frac{d^2\sigma/dQ^2d\nu}{<d\sigma/dQ^2>}$ where $< \frac{d\sigma}{dQ^2} >$ is the integral of $[\frac{d^2\sigma}{dQ^2d\nu}]d\nu$ over all values of ν (for a given value of Q^2).

The right panel of Fig. 1 shows the same QE lepton scattering process, but now also including a final state interaction with another nucleon in the scattering process. This final state interaction modifies the scattering amplitude and therefore can change the kinematics of the final state lepton. In this paper, we refer to it as "fi-

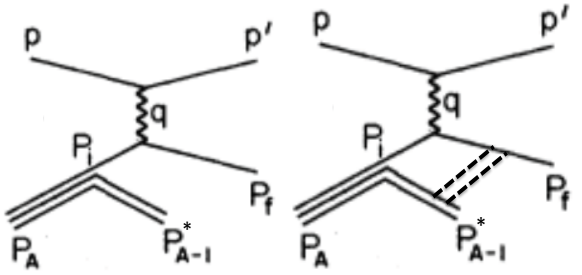


Figure 1: Left: Scattering from an off-shell bound neutron of momentum $\mathbf{P_i} = \mathbf{k}$ in a nucleus of mass A. The on-shell recoil $[A-1]^*$ (spectator) nucleus has a momentum $\mathbf{P^*_{A-1}} = \mathbf{P_s} = -\mathbf{k}$. This process is referred to as the 1p1h process (one proton one hole). Right: The 1p1h process including final state interaction (of the first kind) with another nucleon.

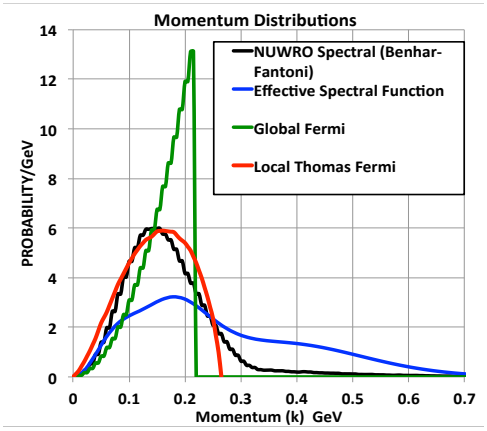


Figure 2: Nucleon momentum distributions in a ^{12}C nucleus for several spectral functions. The curve labeled "Global Fermi" gas is the momentum distribution for the Fermi gas model. The blue line is the momentum distribution for the *effective spectral function* described in this paper.

nal state interaction of the first kind" (FSI). The final state nucleon can then undergo more interactions with other nucleons in the spectator nucleus. These interactions do not change the energy of the final state lepton. We refer to these final state interactions as "final state interaction of the second kind".

In general, neutrino event generators assume that the scattering occurs on independent nucleons which are bound in the nucleus. Generators such as GENIE[2], NEUGEN[3], NEUT[4], NUANCE[5] NuWro [6] and GiBUU[7] account for nucleon binding effects by modeling the momentum distributions and removal energy of nucleons in nuclear targets. Functions that describe the momentum distributions and removal energy of nucleons from nuclei are referred to as spectral functions. Spectral functions describe the initial state.

Spectral functions can take the simple form of a momentum distribution and a fixed removal energy (e.g. Fermi gas[8]), or the more complicated form of a two dimensional (2D) distribution in momentum and removal energy (e.g. Benhar-Fantoni spectral function [9]).

Fig. 2 shows the nucleon momentum distributions in a ^{12}C nucleus for some of the spectral functions that are currently being used. The solid green line is the nucleon momentum distribution for the Fermi gas[8] which is currently implemented in all neutrino event generators. The solid black line is the projected momentum distribution of the Benhar-Fantoni [9] 2D spectral function as implemented in NuWro. The solid red line is the nucleon momentum distribution for the Local-Thomas-Fermi gas (LTF).

It is known that theoretical calculations using spectral functions do not fully describe the shape of the quasielastic peak for electron scattering on nuclear targets . This is because the calculations only model the initial state (shown on the left panel of Fig. 1), and do not account for final state interactions of the first kind (shown on the right panel of Fig. 1) . Because FSI changes the amplitude of the scattering, it modifies the shape of $\frac{1}{\sigma}\frac{d\sigma}{d\nu}$. FSI reduces the cross section at the peak and increases the cross section at the tails of the distribution. In contrast to the spectral function formalism, predictions using the ψ' superscaling formalism[10, 11] fully describe the longitudinal response function of quasielastic electron scattering data on nuclear targets. This is expected since the calculations use a ψ' superscaling function which is directly extracted from the longitudinal component of measured electron scattering QE differential cross sections.

In this communication we present the parameters for a new *effective spectral function* that reproduces the kinematics of the final state lepton predicted by ψ' superscaling. The momentum distribution for this ESF for ^{12}C is shown as the blue line in Fig. 2.

1.1. The ψ' superscaling functions for QE scattering

The ψ scaling variable[10, 11] is defined as:

$$\psi \equiv \frac{1}{\sqrt{\xi_F}} \frac{\lambda - \tau}{\sqrt{(1+\lambda)\tau + \kappa\sqrt{\tau(1+\tau)}}}, \qquad (1)$$

where $\xi_F \equiv \sqrt{1+\eta_F^2} - 1$, $\eta_F \equiv K_F/M_n$, $\lambda \equiv \nu/2M_n$, $\kappa \equiv |\vec{q}|/2M_n$ and $\tau \equiv |Q^2|/4M_n^2 = \kappa^2 - \lambda^2$.

The ψ' superscaling variable includes a correction that accounts for the removal energy from the nucleus. This is achieved by replacing ν with $\nu - E_{\rm shift}$, which

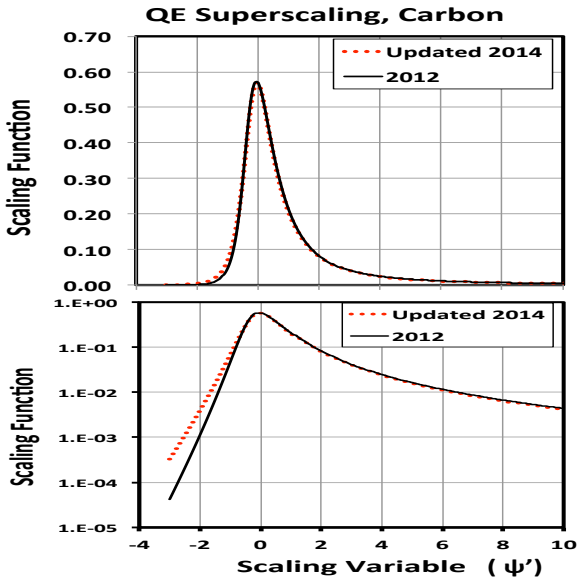


Figure 3: The ψ' superscaling distribution extracted from a fit to electron scattering data used by Bosted and Mamyan [11] (solid black) labeled as 2012, and the superscaling function extracted from a more recent updated fit [12] to data from a large number of quasielastic electron scattering experiments on ^{12}C (dotted red) labeled as 2014). The top panel shows the superscaling functions on a a linear scale. The bottom panel shows the same superscaling functions on a logarithmic scale. The integral of the curve has been normalized to unity.

forces the maximum of the QE response to occur at $\psi' = 0$. QE scattering on all nuclei (except for the deuteron) is described using the same universal superscaling function. The only parameters which are specific to each nucleus are the Fermi broadening parameter K_F and the energy shift parameter $E_{\rm shift}$.

Fig. 3 shows two parametrizations of ψ' superscaling functions extracted from quasielastic electron scattering data on ^{12}C. Shown is the ψ' superscaling distribution extracted from a fit to electron scattering data used by Bosted and Mamyan [11] (solid black line labeled as 2012), and the superscaling function extracted from a recent updated fit[12] to data from a large number of quasielastic electron scattering experiments on ^{12}C (dotted red line labeled as 2014). The top panel shows the superscaling functions on a a linear scale and the bottom panel shows the same superscaling functions on a logarithmic scale.

The ψ' superscaling function is extracted from the longitudinal QE cross section for $Q^2 > 0.3$ GeV^2 where there are no Pauli blocking effects. At very low values of Q^2, the QE differential cross sections predicted by the ψ' superscaling should be multiplied by a Pauli blocking factor $K^{nuclei}_{Pauli}(Q^2)$ which reduces the predicted

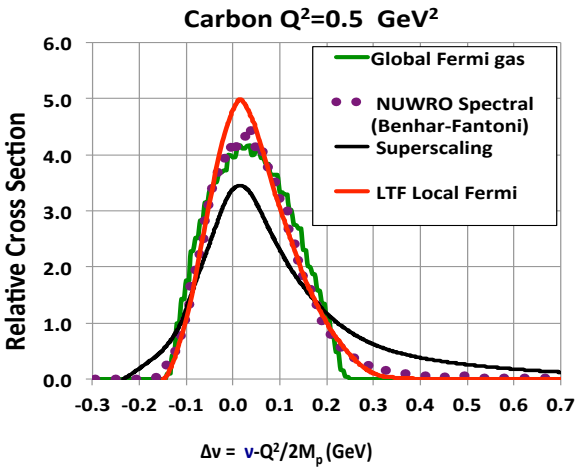


Figure 4: Comparison of the ψ' superscaling prediction (black line) for the normalized $\frac{1}{\sigma}\frac{d\sigma}{d\nu}(Q^2,\nu)$ at Q^2=0.5 GeV^2 for 10 GeV neutrinos on ^{12}C to the predictions of several spectral function models. Here $\frac{1}{\sigma}\frac{d\sigma}{d\nu}(Q^2,\nu)$ is plotted versus $\Delta\nu$ The predictions of the spectral function models are in disagreement with the predictions of ψ' superscaling. .

cross sections at low Q^2. The Pauli suppression factor is given[11] by the function

$$K^{nuclei}_{Pauli} = \frac{3}{4}\frac{|\vec{q}|}{K_F}(1 - \frac{1}{12}(\frac{|\vec{q}|}{K_F})^2) \quad (2)$$

For $|\vec{q}| < 2K_F$, otherwise no Pauli suppression correction is made. Here $|\vec{q}| = \sqrt{Q^2 + \nu^2}$ is the absolute magnitude of the momentum transfer to the target nucleus,

1.2. Comparison of models for quasielastic scattering

Fig. 4 shows predictions for the normalized QE differential cross sections $\frac{1}{\sigma}\frac{d\sigma}{d\nu}(Q^2,\nu)$ for 10 GeV neutrinos on ^{12}C at Q^2=0.5 GeV^2 for various spectral func-

A	$K_F(\psi')$ (GeV)	$E_{\rm shift}(\psi')$ (GeV)
2	0.100	0.001
3	0.115	0.001
$3 < A < 8$	0.190	0.017
$7 < A < 17$	0.228	0.0165
$16 < A < 26$	0.230	0.023
$25 < A < 39$	0.236	0.018
$38 < A < 56$	0.241	0.028
$55 < A < 61$	0.241	0.023
$A > 60$	0.245	0.018

Table 1: Values of Fermi-broadening parameter K_F and energy shift $E_{\rm shift}$ used in the ψ' superscaling prediction for different nuclei. The parameters for deuterium (A=2) are a crude approximation only, and deuterium is treated differently as discussed in reference [1].

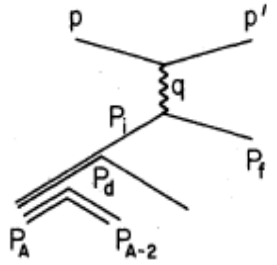


Figure 5: 2p2h process: Scattering from an off-shell bound neutron of momentum $\mathbf{P_i} = -\mathbf{k}$ from two nucleon correlations (quasi-deuteron). The on-shell recoil spectator nucleon has momentum $\mathbf{P_s} = \mathbf{k}$.

tions. Here $\frac{1}{\sigma}\frac{d\sigma}{d\nu}$ is plotted versus $\Delta\nu = \nu - \frac{Q^2}{2M_p}$. The prediction of the ψ' superscaling formalism for $\frac{1}{\sigma}\frac{d\sigma}{d\nu}(Q^2,\nu)$ is shown as the solid black line. The solid green line is the prediction using the "Global Fermi" gas [8]. The solid red line is the prediction using the Local Thomas Fermi gas (LTF) momentum distribution. The dotted purple line is the NuWro prediction using the full two dimensional Benhar-Fantoni[9] spectral function. The predictions of all of these spectral functions for $\frac{1}{\sigma}\frac{d\sigma}{d\nu}(Q^2,\nu)$ are in disagreement with the predictions of the ψ' superscaling formalism.

2. Effective Spectral Function for ^{12}C

2.1. Momentum Distribution

The probability distribution for a nucleon to have a momentum $k = |\vec{k}|$ in the nucleus is defined as

$$P(k)dk = 4\pi k^2 |\phi(k)|^2 dk.$$

For $k < 0.65$ GeV, we parametrize[14] $P(k)$ by the following function:

$$\begin{aligned} P(k) &= \frac{\pi}{4c_0}\frac{1}{N}(a_s + a_p + a_t)y^2 \qquad (3)\\ y &= \frac{k}{c_0}; \qquad a_s = c_1 e^{-(b_s y)^2}\\ a_p &= c_2(b_p y)^2 e^{-(b_p y)^2}; \quad a_t = c_3 y^{\beta} e^{-\alpha(y-2)} \end{aligned}$$

For $k > 0.65$ GeV we set $P(k) = 0$. Here, $c_0 = 0.197$, k is in GeV, N is a normalization factor to normalize the integral of the momentum distribution from k=0 to k=0.65 GeV to 1.0, and P(k) is in units of GeV^{-1}.

2.2. Removal Energy

The kinematics for neutrino charged current quasielastic scattering from a off-shell bound neutron with momentum $\mathbf{k}$ and energy E_n are given by:

$$\begin{aligned} (M'_n)^2 &= (E_n)^2 - Vk^2 \qquad (4)\\ M_p^2 &= (M'_n)^2 + 2E_n\nu - 2|\vec{q}|k_z - Q^2\\ \nu &= E_\nu - E_\mu = \frac{Q^2 + M_p^2 - (M'_n)^2 + 2|\vec{q}|k_z}{(E_n)}\\ V(Q^2) &= 1 - e^{-xQ^2}, \;\; x = 12.04 \qquad (5) \end{aligned}$$

For scattering from a single off-shell nucleon, the term $V(Q^2)$ multiplying k^2 in Equations 4, 6, and 7 should be 1.0. However, we find that in order to make the spectral function predictions agree with ψ' superscaling at very low Q^2 (e.g. $Q^2 < 0.3\ GeV^2$) we need to apply a Q^2-dependent correction to reduce the removal energy, e.g. due to final state interaction (of the first kind) at low Q^2. This factor is given in equation 5. The value of the parameter x=12.04 GeV^{-2} was extracted from the fits at low values of Q^2. As mentioned earlier, $\vec{q}$ is the momentum transfer to the neutron. We define the component of the initial neutron momentum $\mathbf{k}$ which is parallel to $\vec{q}$ as k_z. The expression for E_n depends on the process and is given by Equations 6 and 7 for the 1p1h, and 2p2h process, respectively.

We assume that the off-shell energy (E_n) for a bound neutron with momentum $\mathbf{k}$ can only take two possible values[13]. We refer to the first possibility as the 1p1h process (one proton, one hole in the final state). The second possibility is the 2p2h process(two protons and two holes in the final state).

In our *effective spectral function* model the 1p1h process occurs with probability f_{1p1h}, and the 2p2h process occurs with probability of $1 - f_{1p1h}$. For simplicity, we assume that the probability f_{1p1h} is independent of the momentum of the bound nucleon.

2.2.1. The 1p1h process

The 1p1h process refers to scattering from an independent neutron in the nucleus resulting in a final state proton and a hole in the spectator nucleus. Fig. 1 illustrates the 1p1h process (for $Q^2 > 0.3$ GeV^2), for the scattering from an off-shell bound neutron of momentum $-\mathbf{k}$ in a nucleus of mass A[13]. In the 1p1h process, momentum is balanced by an on-shell recoil $[A-1]^*$ nucleus which has momentum $\mathbf{P^*_{A-1}} = \mathbf{P_s} = \mathbf{k}$ and an average binding energy parameter Δ, where $M_A - M^*_{A-1} = M_n + \Delta$. The initial state off-shell neutron has energy E_n which is given by:

$$\begin{aligned} E_n(1p1h) &= M_A - \sqrt{Vk^2 + (M^*_{A-1})^2}\\ &\approx M_n - \Delta - \frac{Vk^2}{2M^*_{A-1}} \qquad (6) \end{aligned}$$

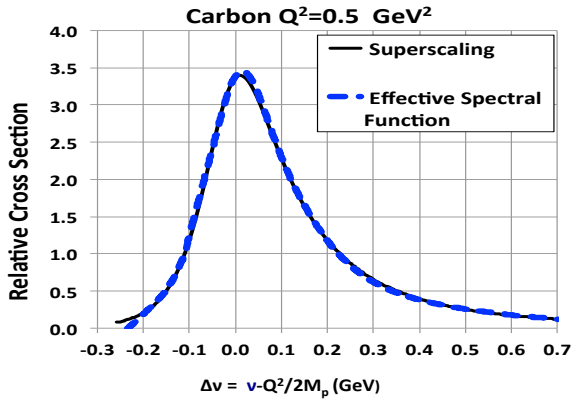


Figure 6: Comparison of the prediction for the normalized QE differential cross section ($\frac{1}{\sigma}\frac{d\sigma}{d\nu}(Q^2,\nu)$) for ^{12}C from the *effective spectral function* to the prediction of ψ' superscaling. The predictions are shown as a function of $\Delta\nu$ at Q^2=0.5 GeV^2. For Q^2=0.5 GeV^2 the prediction of the *effective spectral function* are almost identical to the prediction of ψ' superscaling.

	Benhar-Fantoni	ESF ESF	ESF ESF
Nucl.	^{12}C	^{12}C	^{2}H
Δ (MeV)	2Dspectral	12.5	0.13
f_{1p1h}	2Dspectral	0.808	0
f_{2p2h}	2Dspectral	0.192	1.00
b_s	1.7	2.12	0.413475
b_p	1.77	0.7366	1.75629
α	1.5	12.94	8.29029
β	0.8	10.62	3.621 x10^{-3}
c_1	2.823397	197.0	0.186987
c_2	7.225905	9.94	6.24155
c_3	0.00861524	4.36 x10^{-5}	2.082 x10^{-4}
N	0.985	29.64	10.33

Table 2: A comparison of the parameters that describe the projected momentum distribution for the Benhar-Fantoni spectral function for ^{12}C (2nd column) with the parameters that describe the *effective spectral function* (ESF) (3rd column). Here, Δ is the average binding energy parameter of the spectator one-hole nucleus for the 1p1h process and f_{1p1h} is the fraction of the scattering that occurs via the 1p1h process. For the 2p2h process the average binding energy for the two-hole spectator nucleus is 2Δ. The parameters for the *effective spectral function* for deuterium (^{2}H) are given in the 4th column.

The final state includes a proton and an $[A-1]^*$ nucleus in an excited state because the removal of the nucleon leaves hole in the energy levels of the nucleus.

2.2.2. *The 2p2h process*

In general, there are several processes which result in two (or more) nucleons and a spectator excited nucleus with two (or more) holes in final state:

- Two nucleon correlations in initial state (quasi deuteron) which are often referred to as short range correlations (SRC).
- Final state interaction (of the first kind) resulting in a larger energy transfer to the hadronic final state (as modeled by superscaling).
- Enhancement of the transverse cross sections ("Transverse Enhancement") from meson exchange currents (MEC) and isobar excitation.

In the *effective spectral function* approach the lepton energy spectrum for all three processes is modeled as originating from the two nucleon correlation process. This accounts for the additional energy shift resulting from the removal of two nucleons from the nucleus.

Fig. 5 illustrates the 2p2h process for scattering from an off-shell bound neutron of momentum $-\mathbf{k}$ (for $Q^2 > 0.3$ GeV^2). The momentum of the interacting nucleon in the initial state is balanced by a single on-shell correlated recoil nucleon which has momentum $\mathbf{k}$. The $[A-2]^*$ spectator nucleus is left with two holes. The initial state off-shell neutron has energy E_n given by:

$$E_n(2p2h) = (M_p + M_n) - 2\Delta - \sqrt{Vk^2 + M_p^2} \quad (7)$$

where V is given by eq. 5.

In the *effective spectral function* approach, all effects of final state interaction (of the first kind) are absorbed in the initial state *effective spectral function*. The parameters of the *effective spectral function* are obtained by finding the parameters x, Δ, f_{1p1h}, b_s, b_p, α, β, c_1, c_2, c_3, N and f_{1p1h} for which the predictions of the *effective spectral function* best describe the predictions of the ψ' superscaling formalism for $(1/\sigma)d\sigma/d\nu$ at Q^2 values of 0.1, 0.3, 0.5 and 0.7 GeV^2.

Fig. 6 compares predictions for $\frac{1}{\sigma}\frac{d\sigma}{d\nu}(Q^2,\nu)$ for ^{12}C as a function of $\Delta\nu$ at Q^2=0.5 GeV^2. The prediction of the *effective spectral function* is the dashed blue curve. The prediction of the ψ' superscaling model is the solid black curve. For Q^2=0.5 GeV^2 the prediction of the *effective spectral function* is almost identical to the prediction of ψ' superscaling.

We find that the *effective spectral function* with only the 1p1h process provides a reasonable description of the prediction of ψ' superscaling. Including a contribution from the 2p2h process in the fit improves the agreement and results in a prediction which is almost

Param.	$^{4}_{2}$He	$^{12}_{6}$C	$^{20.8}_{10}$Ne	$^{26.98}_{13}$Al	$^{39.95}_{18}$Ar	$^{55,85}_{26}$Fe	$^{207.2}_{82}$Pb
f_{1p1h}	0.791	0.808	0.765	0.774	0.809	0.822	0.896
b_s	2.14	2.12	1.82	1.73	1.67	1.79	1.52
b_p	0.775	0.7366	0.610	0.621	0.615	0.597	0.585
α	9.73	12.94	6.81	7.20	8.54	7.10	11.24
β	7.57	10.62	6.08	6.73	8.62	6.26	13.33
c_1	183.4	197.0	25.9	21.0	200.0	18.37	174.4
c_2	5.53	9.94	0.59	0.59	6.25	0.505	5.29
c_3	59.0x10^{-5}	4.36 x10^{-5}	221. x10^{-5}	121.5 x10^{-5}	269.0x10^{-5}	141.0 x10^{-5}	9.28x10^{-5}
N	18.94	29.64	4.507	4.065	40.1	3.645	37.96
Δ(MeV)	14.0	12.5	16.6	12.5	20.6	15.1	18.8
E_{shift} ψ'[11]	17.0	16.5	23.0	18.0	28.0	23.0	18.0
K_F ψ'[11]	190	228	230	236	241	241	245
2012	$3 < A < 8$	$3 < A < 8$	$7 < A < 17$	$25 < A < 39$	$38 < A < 56$	$55 < A < 61$	$60 < A$
$\bar{\epsilon}$ Moniz[8]	17.0	25.0	32.0	32.0	28.0	36.0	44.0
K_F Moniz[8]	169	221	235	235	251	260	265
(1971)	$^{6.94}_{3}$Li	$^{12}_{6}$C	$^{24.31}_{12}$Mg	$^{24.31}_{12}$Mg	$^{40.08}_{20}$Ca	$^{58.7}_{28}$Ni	$^{207.2}_{82}$Pb

Table 3: Parameterizations of the *effective spectral function* for various nuclei. Here, Δ is the binding energy parameter, and f_{1p1h} is the fraction of the scattering that occurs via the $1p1h$ process. The parameters for ^{3}He are given in reference [1]. For deuterium (^{2}H) see Table 2, and reference [1]. The best fit values for the binding energy parameter Δ for EFS are similar but not identical to the E_{shift} parameter in the ψ' scaling formalism.[11]. The EFS values for the binding energy parameter Δ are smaller than $\bar{\epsilon}$ extracted within the Fermi gas model from pre 1971 electron scattering data by Moniz[8], probably because these early cross sections were not corrected for coulomb effects.

identical to the prediction of ψ' superscaling.

The parameterizations of the *effective spectral function* for all nuclei from deuterium to lead are given in Tables 2 and 3. As shown in Table 3, the EFS values for the binding energy parameter Δ are smaller than $\bar{\epsilon}$ extracted within the Fermi gas model from pre 1971 electron scattering data by Moniz[8]. This may be because these early cross sections were not corrected for coulomb effects..

3. Conclusion

We present parameters for an *effective spectral function* that reproduce the prediction for $\frac{1}{\sigma}\frac{d\sigma}{d\nu}(Q^2,\nu)$ from the ψ' formalism. We present parameters for a large number of nuclear targets from deuterium to lead.

Since most of the currently available neutrino MC event generators model neutrino scattering in terms of spectral functions, the *effective spectral function* can easily be implemented. For example, it has taken only a few days to implement the *effective spectral function* as an option in recent private versions of NEUT and GENIE. The predictions for QE scattering on nuclear targets using EFS with the inclusion of the the Trasverse Ehancement[1, 15] contribution fully describe electron scattering data by construction.

References

[1] A. Bodek, M. E. Christy, and B. Coopersmith, Xiv:1405.0583v3 (to be published in Eur. Phys. J. C, 2014)

[2] C. Andreopoulos [GENIE Collaboration], Acta Phys. Polon. B 40, 2461(2009), C.Andreopoulos (GENIE), Nucl. Instrum. Meth.A614, 87,2010.

[3] H. Gallagher, (NEUGEN) Nucl. Phys. Proc. Suppl. 112 (2002).

[4] Y. Hayato (NEUT), Nucl Phys. Proc. Suppl.. 112, 171 (2002).

[5] D. Casper (NUANCE) , Nucl. Phys. Proc. Suppl. 112, 161 (2002) (http://nuint.ps.uci.edu/nuance/).

[6] J. Sobczyk (NuWro), PoS NUFACT 08, 141 (2008), C. Juszczak, Acta Phys. Polon. B40 (2009) 2507

[7] T. Leitner, O. Buss, L. Alvarez-Ruso, U. Mosel (GiBUU), Phys. Rev. C79, 034601 (2009) (arXiv:0812.0587).

[8] E. J. Moniz et al. Phys. Rev. Lett. 26, 445(1971); E. J. Moniz, Phys. Rev. 184, 1154 (1969); R. A. Smith and E. J. Moniz, Nucl. Phys. B43, 605 (1972).

[9] O. Benhar and S. Fantoni and G. Lykasov, Eur Phys. J. A 7 (2000), 3, 415; O, Benhar et al., Phys. Rev. C55. 244 (1997).

[10] J.E. Amaro, M.B. Barbaro, J.A. Caballero, T.W. Donnelly, A. Molinari, and I. Sick, Phys. Rev. C 71, 015501 (2005)

[11] P. E. Bosted, V. Mamyan, arXiv:1203.2262.

[12] M. E. Christy, private communication (2014).

[13] A. Bodek, and J. L. Ritchie, Phys. Rev. D23, 1070 (1980). A. Bodek and J. L. Ritchie, Phys. Rev. D24, 1400 (1981).

[14] S. Mishra, (NOMAD collaboration) private communication, fit parameters from E. Iacopini (1997).

[15] A. Bodek, H. S. Budd and M. E. Christy, Eur. Phys. J. C 71, 1726 (2011).